

## ORIGINAL ARTICLE

# Shape and evolution of the fundamental niche in marine *Vibrio*

Arne C Materna<sup>1,8</sup>, Jonathan Friedman<sup>2,8</sup>, Claudia Bauer<sup>3</sup>, Christina David<sup>4</sup>, Sara Chen<sup>1</sup>, Ivy B Huang<sup>1</sup>, April Gillens<sup>5</sup>, Sean A Clarke<sup>6</sup>, Martin F Polz<sup>1</sup> and Eric J Alm<sup>1,2,6,7</sup>

<sup>1</sup>Department of Civil and Environmental Engineering, Massachusetts Institute of Technology, Cambridge, MA, USA; <sup>2</sup>Program in Computational and Systems Biology, Massachusetts Institute of Technology, Cambridge, MA, USA; <sup>3</sup>Institute of Molecular Life Sciences, University of Zürich, Zürich, Switzerland; <sup>4</sup>Harvard Medical School, Harvard University, Boston, MA, USA; <sup>5</sup>Earth and Environmental Science Division, Los Alamos National Laboratory, Los Alamos, NM, USA; <sup>6</sup>Department of Biological Engineering, Massachusetts Institute of Technology, Cambridge, MA, USA and <sup>7</sup>The Broad Institute of MIT and Harvard, Cambridge, MA, USA

**Hutchinson's fundamental niche, defined by the physical and biological environments in which an organism can thrive in the absence of inter-species interactions, is an important theoretical concept in ecology. However, little is known about the overlap between the fundamental niche and the set of conditions species inhabit in nature, and about natural variation in fundamental niche shape and its change as species adapt to their environment. Here, we develop a custom-made dual gradient apparatus to map a cross-section of the fundamental niche for several marine bacterial species within the genus *Vibrio* based on their temperature and salinity tolerance, and compare tolerance limits to the environment where these species commonly occur. We interpret these niche shapes in light of a conceptual model comprising five basic niche shapes. We find that the fundamental niche encompasses a much wider set of conditions than those strains typically inhabit, especially for salinity. Moreover, though the conditions that strains typically inhabit agree well with the strains' temperature tolerance, they are negatively correlated with the strains' salinity tolerance. Such relationships can arise when the physiological response to different stressors is coupled, and we present evidence for such a coupling between temperature and salinity tolerance. Finally, comparison with well-documented ecological range in *V. vulnificus* suggests that biotic interactions limit the occurrence of this species at low-temperature—high-salinity conditions. Our findings highlight the complex interplay between the ecological, physiological and evolutionary determinants of niche morphology, and caution against making inferences based on a single ecological factor.**

*The ISME Journal* (2012) 6, 2168–2177; doi:10.1038/ismej.2012.65; published online 26 July 2012

**Subject Category:** microbial population and community ecology

**Keywords:** interaction; niche; temperature; salinity; stress; zero net growth isoclines

## Introduction

In his often-cited 1957 essay, GE Hutchinson introduced the concept of the fundamental niche as the combination of all environmental conditions (biotic and abiotic) that permit a species to sustain its population in the absence of interference from other species (Hutchinson, 1957). Since that time, the niche concept has been one of the most studied and one of the most debated concepts in theoretical

ecology (Whittaker *et al.*, 1973; Leibold, 1995; Chase and Leibold, 2003; Holt, 2009). Despite its central importance, few empirical studies have been undertaken to map the fundamental niche space associated with non-consumable environmental factors, such as temperature, salinity and pH (Panagou *et al.*, 2005; Hooper *et al.*, 2008). Rather, studies have primarily focused on the effects of multiple consumable environmental resources (for example, nutrients) on inter-species competition (May and MacArthur, 1972; Tilman, 1982; Naeem and Colwell, 1991; Leibold, 1995; Chase and Leibold, 2003).

Hutchinson considered whether niche shapes, that is, the 2-dimensional (2D) cross-section of a pair of environmental factors, could prove informative regarding the physiological response of an organism toward those factors. He deduced that

Correspondence: EJ Alm, Department of Civil and Environmental Engineering, Massachusetts Institute of Technology, 15 Vassar Street, Cambridge, MA 02139, USA.  
E-mail: ejalm@mit.edu

<sup>8</sup>These authors contributed equally to this work.

Received 26 September 2011; revised 12 April 2012; accepted 21 April 2012; published online 26 July 2012

independently acting factors should map out a rectangular fundamental niche, because the maximum tolerance to either factor is independent of the other, and supposed that interactions between factors could lead to more complex shapes. In this way, a species' niche shape reflects the organism's physiological response, for example, whether the stress response pathways for each factor are independent.

In a broader evolutionary context, the population-wide variation in niche shape and the plasticity of these shapes with respect to mutation will have profound effects on how species adapt to new or changing environments. For example, if niche shapes are highly constrained within species, then large changes in environmental factors can lead to significant changes in community composition with many species being displaced. On the other hand, if variation is high within populations, community composition could be robust to large changes in environmental parameters.

In this study, we combine theory and experiment to address the following fundamental questions: (i) What basic classes of 2D niche shapes are anticipated based on considerations of organism physiology? (ii) Which niche shapes are observed? (iii) How does the fundamental niche relate to the environment species typically inhabit? (iv) How do niche shapes vary within and between the populations? Although our scientific questions and theoretical development apply generally to any model system and any environmental factors, we focused our experimental efforts on the salinity–temperature niche of 17 environmental isolates of the bacterial

genus *Vibrio*, representing 11 well-characterized and genetically diverse species, isolated from a range of different environments (Table 1) (Thompson FL *et al.*, 2004a; Thompson JR *et al.*, 2004b; Hunt *et al.*, 2008). Bacteria constitute a convenient model system as their growth can be assayed in high throughput over a range of tightly controlled environmental conditions. The *Vibrio* genus is an excellent model system because it is found in a notable range of environmental temperatures and salinities (Urakawa and Rivera, 2006), which have been shown to be the strongest environmental determinants of microbial community composition (Lozupone and Knight, 2007; Herlemann *et al.*, 2011). Moreover, there is evidence that temperature and salinity are prominent factors in *Vibrio* ecology, population dynamics, physiological stress response and evolution (Kaspar and Tamplin, 1993; McCarthy, 1996; Randa *et al.*, 2004; Garrity *et al.*, 2005; Soto *et al.*, 2009).

## Materials and methods

### Bacterial strains and isolates

The following bacterial strains were used in this study: *V. parahaemolyticus* EB101 (ATCC 17802), *V. fischeri* MJ11 (ATCC 7744), *V. cholerae* N16961 (ATCC 39315), *V. metecus* strains OP6B# and OP3H#, *Listonella* (formerly *Vibrio*) *anguillarum* NCMB 6 (ATCC 19264), *Vibrio* sp. (DAT7222), *Vibrio* sp. MED222 and the *V. splendidus* strains 12B1\*, 12F1\*, 12A10\*, 14B11\*, 12E10\*, *Vibrio* sp. F12\*, *V. crassostreae* 1C5\*, *V. cyclitrophicus* strains 1-273 and Z-264. Strains marked with \* and #

**Table 1** Measured niche shape parameters and strain isolation conditions

| Experiment                               | T <sub>Max</sub><br>(°C) | T <sub>Min</sub><br>(°C) | T <sub>Opt</sub><br>(°C) | Range <sub>Hot</sub><br>(°C) | S <sub>Max</sub><br>(M NaCl) | M <sub>Hot</sub> | Isolation environment                | T <sub>isolation</sub><br>(°C) | S <sub>isolation</sub><br>(M NaCl) |
|--|--------------------------|--------------------------|--------------------------|------------------------------|------------------------------|------------------|--------------------------------------|--------------------------------|------------------------------------|
| <i>V. splendidus</i> 12A10               | 29.16                    | 17.27                    | 21.95                    | 7.21                         | 1.08                         | 1                | PIE-LTER <sup>a</sup>                | 16                             | 0.52–0.58                          |
| <i>V. splendidus</i> 14B11               | 26.62                    | 16.20                    | 21.68                    | 4.94                         | 0.99                         | 0.90             | PIE-LTER                             | 16                             | 0.52–0.58                          |
| <i>V. splendidus</i> 12B1-1 <sup>b</sup> | 27.08                    | 16.27                    | 20.49                    | 6.59                         | 1.07                         | 0.90             | PIE-LTER                             | 16                             | 0.52–0.58                          |
| <i>V. splendidus</i> 12B1-2 <sup>b</sup> | 28.05                    | 20.38                    | 21.71                    | 6.34                         | 1.1                          | 0.83             |                                      |                                |                                    |
| <i>V. splendidus</i> 12F1                | 29.79                    | 15.05                    | 25.50                    | 4.29                         | 1.13                         | 0.77             | PIE-LTER                             | 16                             | 0.52–0.58                          |
| <i>V. splendidus</i> 12E10               | 25.61                    | 15.77                    | 23.79                    | 1.82                         | 1.03                         | 0.84             | PIE-LTER                             | 16                             | 0.52–0.58                          |
| <i>V. sp.</i> MED222                     | 30.15                    | 19.72                    | 25.33                    | 4.82                         | 1.21                         | 0.83             | NW Mediterranean Sea, 1 m depth      | 22                             | NA                                 |
| <i>V. cyclitrophicus</i><br>1–273        | 30.99                    | 21.03                    | 26.71                    | 4.28                         | 1.25                         | 0.87             | PIE-LTER                             | 16                             | NA                                 |
| <i>V. cyclitrophicus</i> Z-264           | 33.15                    | 15.98                    | 22.02                    | 11.13                        | 1.35                         | 0.73             | PIE-LTER                             | 16                             | NA                                 |
| <i>V. sp.</i> F12                        | 30.00                    | 19.70                    | 24.36                    | 5.64                         | 1.17                         | 0.90             | PIE-LTER                             | 16                             | 0.52–0.58                          |
| <i>V. crassostrea</i> 1C5                | 33.22                    | 16.26                    | 26.34                    | 6.88                         | 1.23                         | 0.72             | PIE-LTER                             | 16                             | 0.52–0.58                          |
| <i>V. fischeri</i> MJ11-1 <sup>b</sup>   | 33.16                    | 17.33                    | 25.04                    | 8.12                         | 1.38                         | 0.77             | North sea                            | NA                             | NA                                 |
| <i>V. fischeri</i> MJ11-2 <sup>b</sup>   | 32.48                    | 17.49                    | 25.45                    | 7.03                         | 1.3                          | 0.78             |                                      |                                |                                    |
| <i>V. parahaemolyticus</i>               | 40.35                    | 23.33                    | 29.61                    | 10.74                        | 1.55                         | 0.68             | Dried sardines (shirasu), Japan      | NA                             | NA                                 |
| <i>V. sp.</i> DAT7222                    | 33.96                    | 16.92                    | 27.51                    | 6.45                         | 1.27                         | 0.88             | Aquafarm, Darwin, NT, Australia      | 20–30 <sup>c</sup>             | 0.52 <sup>c</sup>                  |
| <i>Listonella anguillarum</i>            | 31.55                    | 17.09                    | 26.99                    | 4.56                         | 1.17                         | 0.75             | Ulcerous lesion in cod               | NA                             | NA                                 |
| <i>V. metecus</i> OP6B                   | 40.24                    | 19.59                    | 30.94                    | 9.30                         | 1.19                         | 0.64             | Oyster pond, MA, USA                 | 25                             | 0.07                               |
| <i>V. metecus</i> OP3H                   | 36.16                    | 15.88                    | 33.05                    | 3.11                         | 1.32                         | 0.69             | Oyster pond, MA, USA                 | 25                             | 0.07                               |
| <i>V. cholerae</i> N16961                | 41.02                    | 18.50                    | 28.32                    | 12.70                        | 1.28                         | 0.66             | Stool of cholera patient, Bangladesh | NA                             | NA                                 |

<sup>a</sup>Plum Island Long-term Ecological Research.

<sup>b</sup>Biological replicates.

<sup>c</sup>Estimated value.

where isolated from seawater collected at the Plum Island (PIE) Long-term Ecological Research (LTER) site (<http://ecosystems.mbl.edu/pie/data/est/EST.htm>) (Thompson *et al.*, 2005) and Oyster Pond, Woods Hole, MA, USA (Boucher *et al.*, 2011), respectively. *Vibrio* sp. DAT7222 was isolated from aquaculture tanks used to raise marine mud-crab larvae in Australia, Darwin, Northern Territory and was kindly provided by Yan Boucher (Boucher *et al.*, 2006). *Vibrio* sp. MED222 was kindly provided by Jarone Pinhassi, University of Kalmar, Sweden. Note that strains obtained from the ATCC may have undergone periods of replication in constant laboratory conditions.

#### *Cultures and growth conditions*

To ensure clonality of cultures, cells were streaked out to single colonies on solid medium (all analyzed strains lack a swarming motility phenotype on solid medium); subsequently, a single colony was picked for inoculating liquid medium. This isolation step was generally applied before and after storage of a strain at  $-80^{\circ}\text{C}$ . To prepare cultures for  $-80^{\circ}\text{C}$  storage, autoclaved glycerol was added to a final concentration of 25% v/v. Cultures were maintained in tryptic soy broth supplemented with 2% w/v additional sodium chloride (NaCl). For preparation of solid tryptic soy broth medium, Bacto Agar (BD, Franklin Lakes, NJ, USA) was added to a concentration of 1.5% w/v. Cultures were grown at  $22^{\circ}\text{C}$  with gentle shaking (190 r.p.m.). For all experiments on 2D gradients, salinity-adjusted medium (LB-S) was prepared following the protocol for lysogeny broth (LB) medium with the NaCl concentration adjusted as required. We relied solely on NaCl for adjusting the salinity of the growth medium as Stanley and Morita (1968) have shown that NaCl is the most effective salt with respect to restoring normal temperature tolerance in bacteria when replenishing dilute seawater. Other deviations from standard LB medium were that the pH of LB-S medium was adjusted to 8.0 using 1N NaOH and the concentration of agar in solid LB-S was raised from 1.2% to 1.5% w/v.

#### *Preparation of 2D salinity/temperature gradients*

Orthogonal salinity and temperature gradients were established in disposable, non-vented  $241 \times 241 \times 20$  mm bio-assay polystyrene dishes (Nunc, Thermo Fisher Scientific, Roskilde, Denmark). Salinity gradients were established by diffusion between two adjacent medium layers (Panagou *et al.*, 2005) using the following procedure: The dish was tilted by raising one side by 5 mm and a wedge-shaped high salinity base layer was poured, using 170 ml solid LB-S medium containing 2.2 M NaCl. After solidification, the plate was leveled and the top layer was poured using 170 ml solid LB-S medium without additional NaCl (0 M, Supplementary Figure S1).

The gradient was equilibrated for 43 h to ensure diffusion-driven formation of the salinity gradient along one axis of the bio-assay dish. Before inoculation, any residual water (from condensation during cooling of the solid medium) was removed from the surface of the gradient followed by drying for 10 min under sterile laminar air flow.

Stable and reproducible temperature gradients were established using a custom-made device (Supporting Information), into which the bio-assay dish was installed after establishment of a salinity gradient (Supplementary Figure S1).

#### *Inoculation of 2D salinity/temperature gradients*

After colony purification on solid tryptic soy broth medium, cultures were grown overnight in liquid LB-S containing 0.5 M NaCl. After adjusting OD600 to 0.07 using a NanoDrop 1000 (Thermo Scientific, Wilmington, DE, USA) spectrophotometer (1 mm optical path length), the cultures were further diluted in LB-S 0.5 M NaCl to a density of  $6 \times 10^7$  cells ml $^{-1}$ . Cells were then spotted onto the surface of the salinity gradient in a regularly spaced grid of  $24 \times 24$  spots using a 96-well replicator, rather than spread across the surface to avoid cell density effects (for example, colonies that extend into regions that otherwise do not support growth from individual cells). Assuming that each pin of the 96-well replicator transfers a volume of 2–20  $\mu\text{l}$ , the number of cells inoculated onto each spot is estimated to be on the order of  $10^5$ – $10^6$ . The distance of  $\sim 0.9$  mm between neighboring culture spots corresponds to the pins on a 96-well plate replicator.

#### *Data acquisition from 2D salinity/temperature gradients*

Gradient plates were incubated for  $24 \pm 2$  h after inoculation. Zero net growth isoclines (ZNGIs) were determined from the most extreme temperature/salinity values that developed visible colonies within this time frame (Figure 2a), and were used as proxies for niche boundaries. The salinity of all culture spots along the ZNGI and the temperature gradient were measured, and a digital image of the experiment was taken. As temperature gradients proved stable along the salinity axis (Supplementary Figures S3B and S5D), the temperature of culture spots along the ZNGI could be inferred from the temperature gradient, rather than measured for each spot individually. In each experiment, temperature was measured in 1 cm intervals along the temperature axis, using a handheld IR thermometer, with four replicate measurements taken at each point. These measurements were fit to a cubic function, which was then used to infer the temperature at the ZNGI culture spots.

By contrast, the salinity gradients were more variable along the temperature axis (Supplementary Figures S4D and S5B), necessitating the

direct measurement of salinity at each of the ZNGI culture spots.

At each spot, a small core sample was taken, and separated into liquid and solid components by centrifugation for 30 min at 20 800 g. The liquid phase was diluted in deionized water, and ppt salinity measured using a refractometer. A standard curve was used to convert the measured salinities into mol per l NaCl (Supplementary Figure S2). Two duplicate measurements were performed on each core, and their mean was taken as the spot's salinity.

#### *Phylogenetic analysis and independent contrasts*

A phylogenetic tree of the studied strains plus *Escherichia coli* K12 (outgroup for rooting) was constructed based on partial sequences from eight housekeeping genes: *hsp60*, *recA*, *gyrB*, *sodA*, *adh*, *mdh*, *pgi* and *chiA*. Sequences for strains *Vibrio* sp. MED222, *V. parahaemolyticus*, and *V. fischeri* MJ11, and *L. anguillarum* were obtained from complete genomes available on GenBank. For all other strains, partial sequences were obtained during previous studies using multilocus sequencing (Boucher *et al.*, 2011; Preheim *et al.*, 2011, and references therein). Sequences were aligned using MUSCLE (Edgar, 2004), and manually trimmed before concatenating all alignments. A phylogenetic tree was inferred using PhyML (Guindon *et al.*, 2005) with default settings. We note that this tree reflects the strains' evolutionary history, rather than the evolutionary history of particular genes that determine the niche shape.

Felsenstein's (1985) independent contrasts method (Garland *et al.*, 2005) was implemented in the Python programming language, and used to compute correlations between shape parameters and the statistical significance of these correlations. This method is utilized as standard Pearson correlations do not take into account the phylogenetic relationships between strains, which may lead to spurious correlations. The method of independent contrasts circumvents this problem by constructing new, independent variables, which are differences between the parameters of different strains. This method is based on the assumptions that trait evolution is consistent with a neutral Brownian motion model, and that dependencies arise from shared evolutionary ancestry. The validity of these assumptions was assessed using two different methods, as suggested by Garland *et al.* (1992). First, under the model assumptions normalized contrasts are predicted to be independent of the square root of the sum of their branch lengths. This expectation was validated by performing a linear ordinary least-squares fit between these variables. Contrasts that were clear outliers with respect to any of the niche parameters were excluded from further analysis (for example, Supplementary Figure S8). These contrasts corresponded to nodes with

extremely short branch length, and are known to be very sensitive to measurement errors (Ives *et al.*, 2007). Second, the model prediction that contrasts be normally distributed was assessed using the Shapiro-Wilk test for normality (Supplementary Table S1).

## Theory

### *Theory of niche shapes and corresponding classes of stress interactions*

To avoid ambiguity, we formally define the fundamental niche and related terms, as used in this paper. Following Hutchinson, the fundamental niche represents the combination of environmental conditions that permit a species to maintain its populations in the absence of other species. Each combination of permissive conditions can be represented as a point in a high-dimensional space in which each coordinate represents the magnitude of a single environmental factor. The collection of all such points is termed the niche space, and the niche boundary is defined as the curve encapsulating all permissive conditions in the niche space. Equivalently, for a given species, let  $g(E)$  be the species' net growth rate at environmental conditions  $E$ . The fundamental niche corresponds to the set of conditions for which  $g(E) \geq 0$ , and the niche shape to the set of conditions for which  $g(E) = 0$ . As it is not possible to characterize the full (multi-dimensional) extent of the niche space for an organism, we focus on a cross-section in which two non-consumable environmental factors, temperature and salinity, are systematically varied. Changing other environmental factors, such as pH or type of media, can affect the shape of the temperature–salinity fundamental niche as a different cross-section of the full niche space might be measured.

Five basic classes of niche shapes are illustrated in Figure 1. These shapes capture the effect of two non-consumable environmental factors (with levels  $E1$  and  $E2$ ) on a single population, with all other parameters held constant. We assume there exists a unique optimal condition  $\{E1_{opt}, E2_{opt}\}$  that supports the largest sustainable population, and defined the origin to be this condition. The axes thus correspond to deviations from optimal conditions or stress levels. The curves represent niche boundaries, and contained between a curve and the axes is the area corresponding to the fundamental niche. It is important to note that different quadrants represent different types of stress (for example, heat stress vs cold stress), which may have entirely different response pathways and couplings. Thus, the niche shape may vary between quadrants. Figure 1 represents only one quadrant of the niche shape, in which both non-consumable environmental factors are at, or above their optimal level.

We focus on basic niche shapes that can be interpreted in terms of the physiology underlying

the organism's stress response, rather than developing complex models that are able to capture the finer details of niche shapes. To do so, we considered

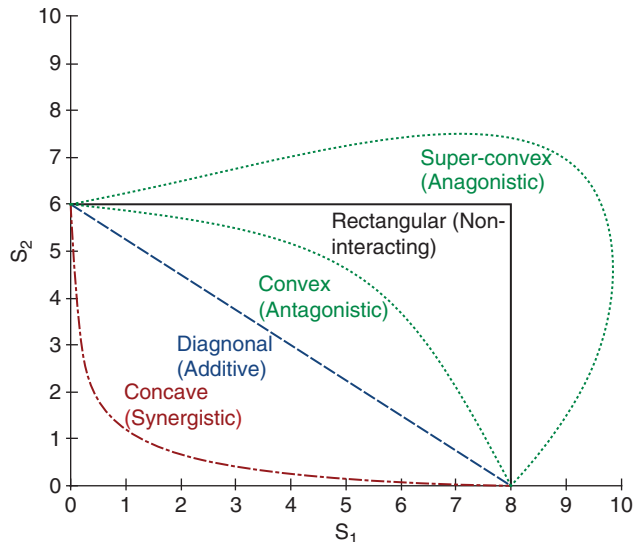


**Figure 1** Five classes of fundamental niche morphology and underlying stress interactions. Axes measure the deviations from the optimal conditions (the origin), that is, the stress due to the environmental factors. The curves represent niche boundaries, with the area contained between a curve and the axes corresponding to the fundamental niche area. Each curve is labeled according to its shape, with the corresponding type of stress interaction indicated in parentheses. Note that only the positive quadrant (both non-consumable environmental factors above their optimal levels) is depicted.

shapes corresponding to zero, linear and non-linear interactions between stresses, with the restrictions that the type of stress interaction is independent of the stress levels (that is, the niche boundary does not cross the additivity line), and that the sign of the curvature of the boundary is constant. An analogous approach is widely used in multicomponent drug therapeutics (Keith *et al.*, 2005; Yeh *et al.*, 2006), where it is known as isobolographic analysis (Gessner, 1995).

These assumptions result in five basic shapes: concave, diagonal, convex, rectangular and super-convex (Figure 1 and Table 2). The simplest case is that of non-interacting stressors, which lead to a rectangular niche shape as the maximal tolerance to either stressor is independent of the level of the other stressor. One way stresses can interact is through both creating demand for a common, limiting cellular resource, such as ATP. That is, some amount of the common cellular resource is dedicated to alleviate the effects of either stress. If the stress level maps to limiting resource consumption in a linear fashion, the fundamental niche boundary will be diagonal. On the other hand, if the resource consumption increases faster or slower than linear with stress levels, niche shapes can be concave or convex, respectively. Other shapes can arise when the concentration or activity of some cellular components (for example, proteins or pathways) affects both stresses simultaneously. These components may not compete for cellular resources,

**Table 2** Basic classes of fundamental niche shapes, and corresponding stress interactions

| Niche shape            | Type of interaction | Description   | Functional form   | Mechanism/example  | M                        |
|------------------------|---------------------|---|---|--|--------------------------|
| Rectangular            | Non-interacting     | Growth rate is determined by the more severe of the two stresses and is completely unaffected by the other stress. As noted by Hutchinson, the corresponding niche shape is rectangular (GE Hutchinson, 1957) | $g(S_1, S_2) = \min\{f_1(S_1), f_2(S_2)\}$ . Note that $f_1(S_1)$ and $f_2(S_2)$ can be any two arbitrary functions   | The cellular mechanisms related to the two stresses, and/or the limiting cellular resources used to alleviate their influence are distinct   | $M = 1$                  |
| Diagonal               | Additive            | Growth rate is determined by a linear combination of the stresses   | $g(S_1, S_2) = f(a_1 * S_1 + a_2 * S_2)$ , where $f(a_1 * S_1 + a_2 * S_2)$ is any arbitrary function of its argument, and $a_1, a_2$ are the amount of common resource required to cope with stresses $S_1$ and $S_2$ , respectively | For each unit of either stress, a common cellular resource is dedicated to alleviate stress effects. The cellular resource may be ATP, a mineral, specific proteins (for example chaperons) and others | $M = 0.5$                |
| Convex<br>Super-convex | Antagonistic        | The combined stress incurred by a combination of two factors is less severe than the stress incurred by only one factor at the equivalent level   | Multiple compatible functional forms  | Concentrations of relevant cellular components under either stress alone are similar   | $0.5 < M < 1$<br>$M > 1$ |
| Concave                | Synergistic         | The combined stress incurred by a combination of the two factors is more severe than the stress incurred by only one factor at the equivalent level   | Multiple compatible functional forms  | Concentrations of relevant cellular components under either stress alone are disparate   | $M < 0.5$                |

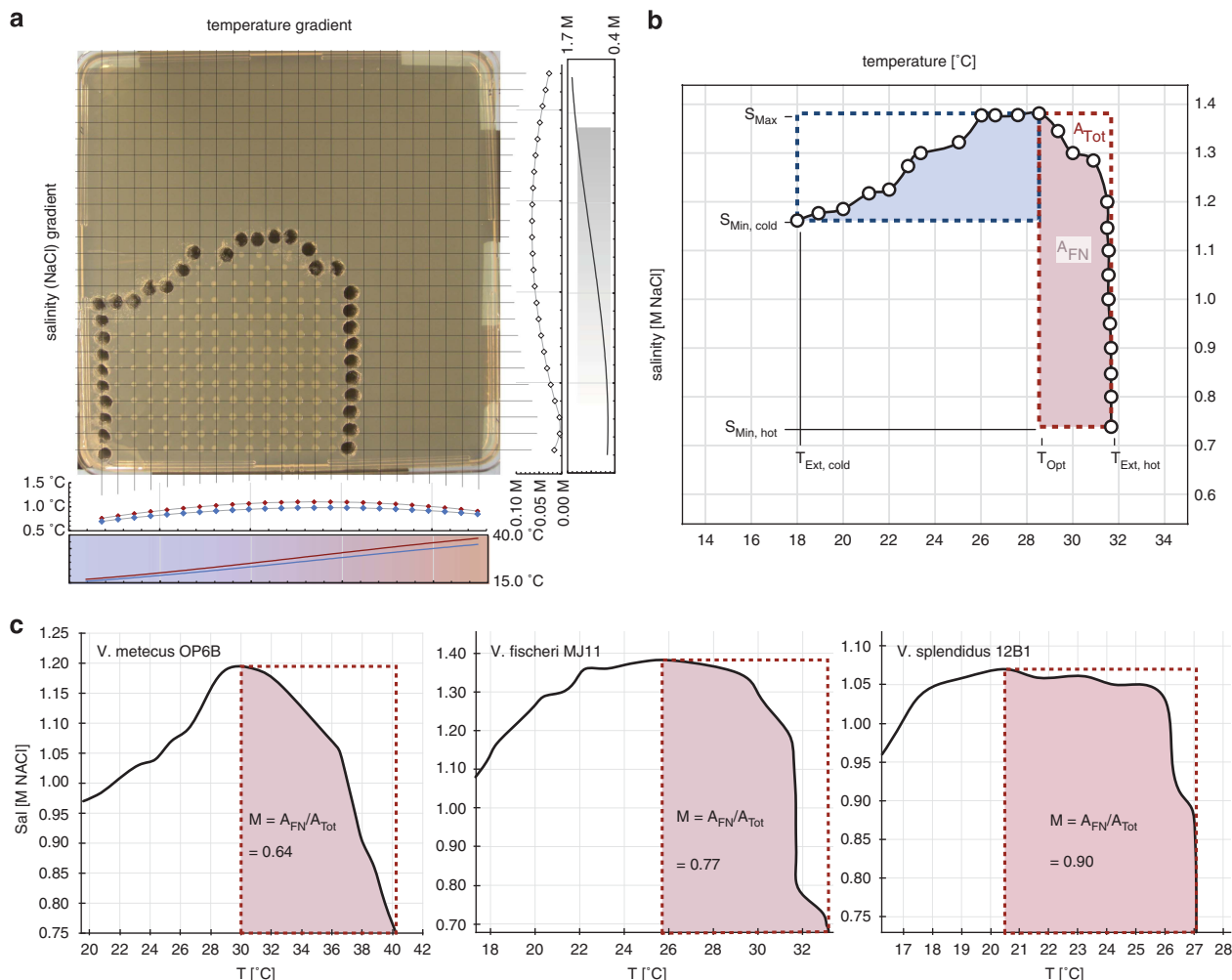


**Figure 2** ZNGI on 2D salinity–temperature gradients. (a) Example of a 2D solid-medium salinity–temperature gradient established in 24 × 24 cm square culture dishes. White spots are bacterial colonies. Dark spots are locations along the estimated ZNGI where salinity was measured directly by destructive coring. The outer plot along the x-axis shows the temperature values (bottom plot, solid lines) and their measurement error (upper plot, diamonds) along the test gradient, when a low- (blue) or high- (red) temperature range setup was employed. Corresponding plots for salinity are shown along the y-axis (for details see Materials and methods, Supporting Information). (b) Example of a measured ZNGI (open circles) and niche shape parameters. Parameters are shown for both the high temperature and low-temperature quadrants, though our analysis focuses on the high temperature quadrant (see main text).  $T_{\text{Ext, hot}}$  ( $T_{\text{Max}}$ )—highest permissible temperature.  $T_{\text{Ext, cold}}$ —lowest permissible temperature.  $T_{\text{Opt}}$ —optimal temperature (as defined in main text).  $S_{\text{Max}}$ —highest permissible salinity.  $S_{\text{Min}}$ —lowest permissible salinity.  $A_{\text{FN}}$ —area of the fundamental niche (shaded).  $A_{\text{Tot}}$ —area of the fundamental niche if the stresses acted independently. (c) Examples of the three classes of niche shapes observed: diagonal, convex and rectangular (from left to right). Shaded areas correspond to the niche area in the high-temperature quadrant.

but instead change the physicochemical properties of the cell. For example, the permeability of the cell membrane is altered by the concentration of porins, and can influence the effect of multiple stresses. Super-convex shapes can arise if the effects of one stress alleviate the effects of another, and concave shapes can result if the optimal activity of these cellular components is different.

These basic niche shapes are a simplification and an idealization, which is not expected to be precisely reproduced in observed niche shapes. Rather, they enable the identification of the dominant features of stress response physiology. For instance, though stress response is typically multifaceted, if a nearly diagonal shape is observed

(for example, Figure 2c), it is likely that the main response pathways of the two stresses compete for the same cellular resource.

## Results

### Measurement of 2D salinity–temperature gradients

We designed an inexpensive platform to create 2D orthogonal gradients of temperature and salinity on solid media, which allowed estimation of niche shapes realized in natural populations and their comparison to our simple theoretical model. We focused on the high-temperature/high-salinity quadrant, because our experimental apparatus did not allow us to examine sufficiently low temperatures

for many strains. In addition, we found that upon removal of the temperature stress, new colonies developed at the cold-temperature region, whereas no new colonies form at the high-temperature region within an additional 24 h, consistent with previous studies showing resuscitation following a temperature increase (McDougald and Kjelleberg, 2006). Therefore, at low temperatures there was ambiguity between no growth and slow growth phenotypes, although the effect of higher temperatures was cell death, making analysis more straightforward. Our motivation to focus on the high-salinity region was to achieve greater resolution and to be able to use the same rich medium for all strains. Assaying lower salinities would require using strain-specific media, which may differentially affect niche morphology, convoluting niche comparisons.

Niche morphology was quantified using the following parameters: highest permissive temperature ( $T_{\text{Max}}$ ), highest permissive salinity ( $S_{\text{Max}}$ ), optimal temperature ( $T_{\text{Opt}}$ ) and niche morphology index ( $M$ ). The niche morphology index, which summarizes how interactions between stressors affect niche boundaries, was defined to objectively classify the different niche shapes.  $M$  is defined as the area spanned by the niche divided by the area of the rectangular niche that would be observed had the two stressors been acting independently (Figure 2). Table 2 illustrates how  $M$  values correspond to different classes of niche shape: concave— $M < 0.5$ ; diagonal— $M = 0.5$ ; convex— $0.5 < M < 1$ ; rectangular— $M = 1$ ; super-convex— $M > 1$ . We note that although  $S_{\text{Opt}}$  was outside the measured salinity range, the inferred  $M$  values are representative of those of the full high-temperature/high-salinity quadrant, as long as the class of niche shape is consistent in this quadrant (note that no such switches were observed in the measured range of any of the strains).

In general,  $T_{\text{Opt}}$  can be a function of salinity and requires detailed growth curves at each position to measure directly. We avoided this added complexity by approximating  $T_{\text{Opt}}$  using two independent methods: (i) we took  $T_{\text{Opt}}$  as the temperature that allows growth in the highest salinity ( $S_{\text{Max}}$ ), and (ii) we defined  $T_{\text{Opt}}$  as the midpoint of the range of temperatures in which the largest colonies formed. We note that the first approach is not applicable to super-convex shapes. However, the second method, which is capable of detecting super-convex shapes, yielded nearly identical results, with no super-convex shapes. Therefore, we report results based on the first, more straightforward approach.

#### Observed niche shapes

$M$  values fell in a narrow range between 0.64 and 1.00, and the observed niche shapes were all convex, ranging from nearly diagonal to nearly rectangular (Table 1, Figure 3). No concave or super-convex shapes were observed. Niche shape

parameters for all strains are summarized in Table 1, and niche shapes of all strains are depicted in Supplementary Figure S6. We note that classes of niche shapes in the low-temperature/high-salinity quadrant are consistent with those of the high-temperature/high-salinity quadrant (Supplementary Figure S7), and were excluded solely because we have less confidence in their accuracy, as detailed in the previous section.

Maximal permissible temperatures, ranging from 25 °C to 41 °C, were consistent with realistic environmental conditions, whereas permissible salinities, ranging from 0.99 M NaCl to 1.55 M NaCl, far exceeded that typical of marine environments of ~0.6 M NaCl (Emerson and Hedges, 2008). Moreover, though the conditions in which strains typically inhabit agrees well with the strains' temperature tolerance, they are negatively correlated with the strains' salinity tolerance (Figure 3). This is exemplified by the fact that *V. cholerae* strains from warm estuarine and freshwater environments display high temperature and salt tolerance, whereas *V. splendidus* strains from a colder marine environment have a markedly lower temperature and salt tolerance.

Additionally, we observe that the various niche parameters do not vary independently. Salinity and temperature tolerance are positively correlated with each other, and negatively correlated with  $M$  values (Figure 3). Thus, strains that display niche shapes consistent with independent responses to both stressors generally have lower overall tolerance to those stressors. By contrast, strains with high tolerances to a single stressor tend to also have a high tolerance to the other stressor, and have a niche shape consistent with the existence of coupling between the stress responses. Although these trends appear highly significant, spurious correlations between independently evolving factors can arise because of the phylogenetic structure of the data. To control for phylogenetic effects, we used Felsenstein's method of independent contrasts (Felsenstein, 1985; Garland *et al.*, 2005) to compute correlations between niche shape parameters and evaluate their significance. Even after accounting for the phylogeny, the observed trends remained statistically significant:  $T_{\text{Max}}$  and  $S_{\text{Max}}$  had a correlation of 0.86 ( $P$ -value  $7.2e - 4$ );  $T_{\text{Max}}$  and  $M_{\text{hot}}$  had a correlation of  $-0.62$  ( $P$ -value  $2.7e - 2$ );  $S_{\text{Max}}$  and  $M_{\text{hot}}$  had a correlation of  $-0.56$  ( $P$ -value  $4.6e - 2$ ).

#### Evolution of the fundamental niche

Comparison of niche shape across 17 strains provides a clear answer to the question of whether the majority of variation in niche shape occurs within or between species. Inspection of Figure 3c shows that niche shapes tend to be more similar between closely related strains, with very limited or no qualitative niche morphology changes occurring within species. For example, the cluster of

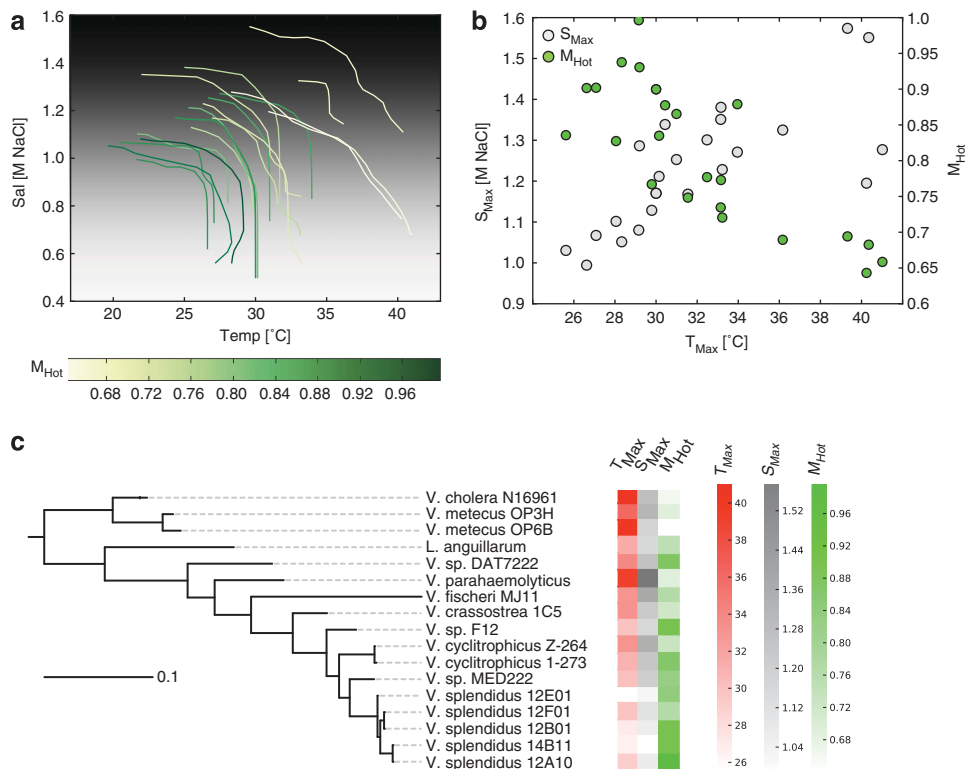


**Figure 3** Evolution of the fundamental niche. **(a)** ZNGIs of all strains at the high-temperature/high-salinity quadrant, colored by  $M$  values. ZNGIs tend to be located along the diagonal from the bottom-left corner to the top-right corner, indicating a correlation between temperature and salinity tolerance. Additionally, as strains become more tolerant their niche shape varies from rectangular to diagonal (decreasing  $M$  value). **(b)** Maximal permissive temperature ( $T_{\text{Max}}$ ) vs maximal permissive salinity ( $S_{\text{Max}}$ ) and  $M$ -value. Each point represents the values measured for a single strain. Note that the correlations were calculated using Felsenstein's method of independent contrasts (see main text). **(c)** MLSA phylogenetic tree of all strains. Corresponding values of  $T_{\text{Max}}$ ,  $S_{\text{Max}}$  and  $M$  are given by the color bars to the right.

*V. splendidus* isolates shows low tolerance to high temperatures and salinities, and almost rectangular niche shapes (high  $M$ ), although the *V. cholerae/metecus* isolates display high temperature and salinity tolerances and nearly diagonal niche shapes (low  $M$ ). The average difference in niche parameters measured between these groups exceeds the within-population variation by a factor of 2.5 (for  $S_{\text{max}}$ ) to 5 (for  $T_{\text{max}}$ ).

## Discussion

The fundamental niche captures the range of environmental conditions in which a species can persist in isolation. However, as natural communities typically comprise numerous interacting species, the extent to which the fundamental niche is relevant to the ecology of natural communities is unclear and warrants further investigation. In this study, we show that all studied strains could tolerate salinities that are unlikely to be ecologically relevant, indicating that, in this dimension, their fundamental niche is far broader than their ecological range. In addition, Randa et al. (Randa et al., 2004) found that *V. vulnificus* usually occurs in

low-salinity environments, but, as the temperature increases, it can expand its range into higher salinity environments. In light of our results, the fact that *V. vulnificus* is rare at saline, low-temperature environments is likely a consequence of biotic interactions, such as competitive exclusion or predation, rather than an inherent inability to thrive at these conditions. Thus, *V. vulnificus*' realized ecological range is a limited section of its fundamental niche.

Temperature and salinity tolerances are positively correlated across all strains in the study despite the fact that these factors are negatively correlated in some of the environments the strains were isolated from (for example, *V. metecus* strains from a warm, low-salinity environment in contrast to *V. splendidus* strains from a colder, saline marine environment). These results indicate that salinity and temperature tolerance mechanisms may be coupled at the molecular level, consistent with the findings of previous studies demonstrating that pre-exposure to osmotic stress increased the tolerance to heat stress in *V. vulnificus* (Rosche et al., 2005). Such coupling may result from temperature and salinity responses using common molecular pathways such as the SOS response pathway, the heat-shock



response pathway and the general stress response pathway (Hengge-Aronis, 2002; Diez-Gonzalez and Kuruc, 2009). However, Rosche *et al.* (2005) have demonstrated that the cross-protection between osmolarity and heat in *V. vulnificus* is independent of rpoS, the master regulator of the general stress response mechanism, and were unable to elucidate the origin of this cross-protection.

An alternative potential mechanism for coupling between stress responses is partitioning of cellular resources between different stress response pathways. In the simplest (linear) model, a cell's tolerance would be a function of the sum of the two stress levels, leading to diagonal niche shapes ( $M \sim 0.5$ ). Remarkably, we observe an inverse correlation between stress tolerance and  $M$  values that remains significant even after controlling for phylogeny. Together with the unexpected positive correlation between the two stress tolerances, this correlation suggests a model in which the temperature and salinity response pathways are coupled, and moreover, that they compete for common cellular resources (for example, ATP).

Temperature adaptation may explain the incongruence between salinity tolerance and environmental salinity. As maximal temperatures are consistent with conditions at environments strains typically occur in, and strains can tolerate a much wider range of salinities than is ecologically relevant, it is possible that heat tolerance is under much stronger selection than salinity tolerance. Under this hypothesis, heat tolerance is set by the environmental conditions, which in turn affects salinity tolerance, which is mechanistically coupled to it. Thus, like heat tolerance, salinity tolerance is predicted to be correlated with environmental temperature, rather than environmental salinity. This is indeed the case in our data.

The potential for coupling between stressors cautions against making inferences based on individual stress tolerance phenotypes, as the results could be at odds with ecology. In fact, we cannot rule out coupling along other unmeasured dimensions (for example, nutrient levels, pH), nor can we rule out that these factors (rather than temperature) may be driving salinity and/or temperature tolerance levels. Nonetheless, these results indicate that meaningful work linking physiological, ecological and evolutionary aspects of niche theory will require an appreciation of the nuances of a multi-dimensional and potentially highly coupled niche space.

## References

Boucher Y, Cordero OX, Takemura A, Hunt Dana E, Schliep K, Baptiste E *et al.* (2011). Local mobile gene pools rapidly cross species boundaries to create

endemism within global *Vibrio cholerae* populations. *mBio* **2**: e00335–10.

Boucher Y, Nesbø CL, Joss MJ, Robinson A, Mabbutt BC, Gillings MR *et al.* (2006). Recovery and evolutionary analysis of complete integron gene cassette arrays from *Vibrio*. *BMC Evol Biol* **6**: 3.

Chase JM, Leibold MA. (2003). *Ecological Niches: Linking Classical and Contemporary Approaches*. University of Chicago Press: Chicago.

Diez-Gonzalez F, Kuruc J. (2009). Molecular mechanisms of microbial survival in foods. In: Jaykus L-A, Wang HH, Schlesinger LS (eds). *Food-Borne Microbes: Shaping the Host Ecosystem*. ASM Press: Washington, DC, pp 135–159.

Edgar RC. (2004). MUSCLE: a multiple sequence alignment method with reduced time and space complexity. *BMC Bioinformatics* **5**: 113.

Emerson S, Hedges J. (2008). *Chemical Oceanography and the Marine Carbon Cycle*. Cambridge University Press: Cambridge.

Felsenstein J. (1985). Phylogenies and the comparative method. *Am Nat* **125**: 1–15.

Garland T, Bennett AF, Rezende EL. (2005). Phylogenetic approaches in comparative physiology. *J Exp Biol* **208**: 3015–3035.

Garland T, Harvey PH, Ives AR. (1992). Procedures for the analysis of comparative data using phylogenetically independent contrasts. *Syst Biol* **41**: 18–32.

Garrity GM, Brenner DJ, Krieg NR. (2005). *Bergey's Manual Of Systematic Bacteriology*. Springer: New York.

Gessner P. (1995). Isobolographic analysis of interactions: an update on applications and utility. *Toxicology* **105**: 161–179.

Guindon S, Lethiec F, Duroux P, Gascuel O. (2005). PHYML Online—a web server for fast maximum likelihood-based phylogenetic inference. *Nucleic Acids Res* **33**: W557–W559.

Hengge-Aronis R. (2002). Signal transduction and regulatory mechanisms involved in control of the sigma(S) (RpoS) subunit of RNA polymerase. *Microbiol Mol Biol Rev* **66**: 373–395.

Herlemann DP, Labrenz M, Jurgens K, Bertilsson S, Waniek JJ, Andersson AF. (2011). Transitions in bacterial communities along the 2000km salinity gradient of the Baltic Sea. *ISME J* **5**: 1571–1579.

Holt RD. (2009). Bringing the Hutchinsonian niche into the 21st century: Ecological and evolutionary perspectives. *Proc Natl Acad Sci USA* **106**: 19659–19665.

Hooper HL, Connon R, Callaghan A, Fryer G, Yarwood-Buchanan S, Biggs J *et al.* (2008). The ecological niche of *Daphnia magna* characterized using population growth rate. *Ecology* **89**: 1015–1022.

Hunt DE, David LA, Gevers D, Preheim SP, Alm EJ, Polz MF. (2008). Resource partitioning and sympatric differentiation among closely related bacterioplankton. *Science* **320**: 1081–1085.

Hutchinson GE. (1957). Concluding remarks. *Cold Spring Harbor Symp Quant Bio* **22**: 415–427.

Ives AR, Midford PE, Garland T. (2007). Within-species variation and measurement error in phylogenetic comparative methods. *Syst Biol* **56**: 252–270.

Kaspar CW, Tamplin ML. (1993). Effects of temperature and salinity on the survival of *Vibrio vulnificus* in seawater and shellfish. *Appl Environ Microbiol* **59**: 2425.

- Keith CT, Borisy AA, Stockwell BR. (2005). Multicomponent therapeutics for networked systems. *Nat Rev Drug Discov* **4**: 71–78.
- Leibold MA. (1995). The niche concept revisited: mechanistic models and community context. *Ecology* **76**: 1371–1382.
- Lozupone CA, Knight R. (2007). Global patterns in bacterial diversity. *Proc Natl Acad Sci* **104**: 11436–11440.
- May R, MacArthur R. (1972). Niche overlap as a function of environmental variability. *Proc Natl Acad Sci USA* **69**: 1109–1113.
- McCarthy SA. (1996). Effects of temperature and salinity on survival of toxigenic *Vibrio cholerae* O1 in seawater. *Microb Ecol* **31**: 167–175.
- McDougald D, Kjelleberg S. (2006). Adaptive responses to Vibrios. In: Thompson F, Austin B, Swings J (eds). *The Biology of Vibrios*. ASM Press: Washington, DC, pp 133–155.
- Naeem S, Colwell RK. (1991). Ecological consequences of heterogeneity of consumable resources. In: Kolasa J, Pickett STA (eds). *Ecological Heterogeneity*. Springer-Verlag: New York, pp 224–255.
- Panagou EZ, Skandamis PN, Nychas G-JE. (2005). Use of gradient plates to study combined effects of temperature, pH, and NaCl concentration on growth of *Monascus ruber* van Tieghem, an Ascomycetes fungus isolated from green table olives. *Appl Environ Microbiol* **71**: 392–399.
- Preheim SP, Timberlake S, Polz MF. (2011). Merging taxonomy with ecological population prediction in a case study of Vibrionaceae. *Appl Environ Microbiol* **77**: 7195–7206.
- Randa MA, Polz MF, Lim E. (2004). Effects of temperature and salinity on *Vibrio vulnificus* population dynamics as assessed by quantitative PCR. *Appl Environ Microbiol* **70**: 5469–5476.
- Rosche TM, Smith DJ, Parker EE, Oliver JD. (2005). RpoS involvement and requirement for exogenous nutrient for osmotically induced cross protection in *Vibrio vulnificus*. *FEMS Microbiology Ecology* **53**: 455–462.
- Soto W, Gutierrez J, Remmenga MD, Nishiguchi MK. (2009). Salinity and temperature effects on physiological responses of *Vibrio fischeri* from diverse ecological niches. *Microb Ecol* **57**: 140–150.
- Stanley SO, Morita RY. (1968). Salinity effect on the maximal growth temperature of some bacteria isolated from marine environments. *J Bacteriol* **95**: 169–173.
- Thompson FL, Iida T, Swings J. (2004a). Biodiversity of vibrios. *Microbiol Mol Biol Rev* **68**: 403.
- Thompson JR, Pacocha S, Pharino C, Klepac-Ceraj V, Hunt DE, Benoit J *et al*. (2005). Genotypic diversity within a natural coastal bacterioplankton population. *Science* **307**: 1311–1313.
- Thompson JR, Randa MA, Marcelino LA, Tomita-Mitchell A, Lim E, Polz MF *et al*. (2004b). Diversity and dynamics of a North Atlantic Coastal *Vibrio* community. *Appl Environ Microbiol* **70**: 4103–4110.
- Tilman D. (1982). *Resource Competition and Community Structure*. Princeton University Press: Princeton.
- Urakawa H, Rivera I. (2006). Aquatic environment. In: Thompson F, Austin B, Swings J (eds) *The Biology of Vibrios*. ASM Press: Washington, DC, pp 175–189.
- Whittaker RH, Levin SA, Root RB. (1973). Niche, habitat, and ecotope. *Am Nat* **107**: 321–338.
- Yeh P, Tschumi AI, Kishony R. (2006). Functional classification of drugs by properties of their pairwise interactions. *Nat Genet* **38**: 489–494.

Supplementary Information accompanies the paper on The ISME Journal website (<http://www.nature.com/ismej>)